OXFORD
SOT | Society of Toxicology
www.toxsci.oxfordjournals.org

TOXICOLOGICAL SCIENCES, 148(2), 2015, 594–602

doi: 10.1093/toxsci/kfv208
Advance Access Publication Date: September 22, 2015
Research Article

Quantification of Low-Level Drug Effects Using Real-Time, *in vitro* Measurement of Oxygen Consumption Rate

Adam Neal,* Austin M. Rountree,* Craig W. Philips,† Terrance J. Kavanagh,‡ Dominic P. Williams,§ Peter Newham,§ Gamal Khalil,¶ Daniel L. Cook,¶ and Ian R. Sweet*,¶,1

*Department of Medicine, University of Washington, Seattle, Washington, 98195; †Center for Commercialization, University of Washington, Seattle, Washington 98195; ‡Department of Environmental and Occupational Health Sciences, University of Washington, Seattle, Washington 98105; §Department of Drug Safety and Metabolism, AstraZeneca, Cambridge Science Park, Milton Road, Milton, Cambridge CB4 0FZ, UK; and ¶EnTox Sciences, LLC, Mercer Island, Washington 98040.

[1]To whom correspondence should be addressed at Department of Medicine, University of Washington, Seattle, Washington, 98195. Fax: 206 543 3567. E-mail: isweet@u.washington.edu

ABSTRACT

There is a general need to detect toxic effects of drugs during preclinical screening. We propose that increased sensitivity of xenobiotics toxicity combined with improved *in vitro* physiological recapitulation will more accurately assess potentially toxic perturbations of cellular biochemistry that are near *in vivo* pharmacological exposure levels. Importantly, measurement of such cytopathologies avoids activating mechanisms mediating toxicity at suprapharmacologic levels not relevant to *in vivo* effects. We present a sensitive method to measure changes in oxygen consumption rate (OCR), a well-established parameter reflecting a potential hazard, in response to exposure to pharmacologic levels of drugs using a flow culture system and state of the art oxygen sensing system. We tested metformin and acetaminophen on rat liver slices to illustrate the method. The features of the method include continuous and very stable measurement of OCR over the course of 48 h in liver slices in a continuous flow chamber with the ability to resolve changes as small as 0.3%/h. Kinetic modeling of metformin inhibition of OCR over a wide range of concentrations revealed both a slow and fast mechanism, where the fast mechanism activated only at concentrations above 0.6 mM. For both drugs, small amounts of inhibition were reversible, but higher decrements were irreversible. Overall the study highlights the advantages of measuring low-level toxicity so as to avoid the common extrapolations made about drug toxicity based on effects of drugs tested at suprapharmacologic levels.

Key words: oxygen consumption rate; drug toxicity; metformin; acetaminophen; liver slices; mathematical modeling

A Critical Need For Improved Drug Testing

Toxic side effects of drugs harm patients and their families, and cost pharmaceutical companies billions of dollars in lawsuits, lost business and squandered research, and development effort. Highly visible, late-stage drug attrition, and failures, particularly during clinical testing and distribution, are only part of the picture. One of the great challenges facing the pharmaceutical industry is the early detection of such toxicities prior to very expensive preclinical animal safety and clinical trials (Astashkina *et al.*, 2012; McKim, 2010; Zemmel and Sheikh, 2010). However, detecting all potentially harmful side effects during drug development, especially those that occur at levels close to prescribed levels, is a challenge for currently available technologies. We contend there is a need for a preclinical

toxicity testing method that can provide unprecedented dose-sensitivity (eg, well below cytotoxic doses), reveal a broad range of cytopathologies (eg, beyond a specific biochemical endpoint), and define important pharmacokinetic effects (eg, reversibility). We achieve these unprecedented capabilities using critical refinements to our previously published methods (Sweet *et al.*, 2002a,b) for a highly sensitive measure of tissue oxygen uptake during long-term, flow-through culture capable of measuring small gradual changes in oxygen consumption. As previously discussed (Sweet *et al.*, 2004; Sweet and Gilbert, 2006), we interpret decrements and increments of oxygen consumption rate (OCR) as evidence of perturbed cell biochemistry that may signal cytopathologies warranting further characterization prior to drug development. Here, we describe recent and critical technical improvements to achieve a combination of sensitivity and stability to yield fundamental and quantitative characterization of drug effects and their reversibility as a critical tool for pharmaceutical product development. For illustrative purposes, we applied the methods to metformin and acetaminophen, 2 safe drugs that are widely used, but which have effects that allowed the features of the approach to be assessed. (More toxic drugs should yield similar data except that their dose response curves should be shifted to the left.) Analysis of the data showed that evaluating high levels of toxicity activated multiple mechanisms, high sensitivity of the method resolved mechanisms likely to occur *in vivo*, and the method provides unique *in vitro* data useful in drug screening.

MATERIALS AND METHODS

Materials. Williams' E Media (Sigma-Aldrich, St. Louis, Missouri) supplemented with 10% heat-inactivated fetal bovine serum (Atlanta Biologicals, Lawrenceville, Georgia), 2 mM glutamine and 1% Pen/strep and 20 mM HEPES (Research Organics, Cleveland, Ohio) was used for all perifusion analysis. Metformin and acetaminophen were obtained as a generous gift from Astra-Zeneca, London, UK and was added to the perifusion media as indicated. The oxygen-sensitive dye, Pt(II) meso-Tetra(N-Methyl-4-Pyridyl)Porphine Tetrachloride, was purchased from Frontier Scientific (Logan, Utah).

Animals. Liver slices were harvested from Sprague–Dawley rats (≈250 g, Charles River) anesthetized by intraperitoneal injection of sodium pentobarbital (35 mg/230 g rat). All procedures were approved by the University of Washington Institutional Animal Care and Use Committee.

Preparation of rat liver slices. Whereas we have developed our flow culture system using a variety of tissue types (Du *et al.*, 2013; Han *et al.*, 2012; Sahni *et al.*, 2010; Sweet *et al.*, 2005, 2008; Weydt *et al.*, 2006), we chose the rat liver slice preparation as relevant for pharmaceutical development. All procedures were performed under aseptic conditions in a laminar flow hood. After anesthesia was induced, the midsection was opened up to expose the liver. A piece of liver lobe (size = 4 cm^3) was removed with surgical scissors. The piece was laid out on a petri dish containing William's E Media, and after cutting away a layer of capsule, multiple slices were diced [~0.25 × 1 mm (mass = 1–2 mg per piece)] with a scalpel. Four of the pieces were loaded in to the perifusion chamber for each analysis. After the end of each experiment, the liver samples were weighed and OCR measurements were normalized to this mass.

Flow culture system. The flow system is designed to maintain tissue under conditions similar to a CO_2 incubator, and was based on the original design described previously (Sweet *et al.*, 2002a,b), but with a number of important modifications designed to improve performance and accuracy (see Fig. 1 for complete description of parts). Media was pumped through the chamber at a flow rate of 80–100 μl/min using an 8-channel Watson-Marlow peristaltic pump (Model 205U, Wilmington, Massachusetts), which allowed very accurate and stable flow rate control (CV = 1–2 percent) with little pulsatility. In order to minimize bubble formation in the bicarbonate based media, a 2-compartment plexiglass housing was constructed. The bottles of media were placed in 1 compartment, where temperature was maintained at 42°C using a Chromolox 2110 heating unit/fan in order to ensure that media always moved from high to lower temperature thereby avoiding a critical driving force for degassing. The 2 compartments were separated by a plexiglass divider, and the second compartment containing the gas equilibration system and the perifusion chambers was filled with water maintained at 37°C by use of an immersion heater (VWR, Radnor, Pennsylvania). To control gas tension in the perifusate, just prior to entering the tissue chambers, the perifusate flowed through an artificial lung consisting of 24 cm of gas-permeable silastic tubing (1.6 mm i.d., 2.4 mm o.d.) loosely coiled in a 10 cm long glass tube (diameter = 3 cm) that was continuously supplied with 10 ml/min of 21% oxygen and 5% CO_2 through ports in the rubber plugs. Eight chambers were perifused in parallel. All surfaces coming into contact with media including tubing, tubing connectors, tissue chambers and media bottles were sterilized using an autoclave, and the flow conduit systems were pre-assembled in a laminar flow hood. Drugs were administered to the inflow by spiking the agent into the media bottles using a P200 pipet.

Continuous detection of oxygen tension. Oxygen tension was measured by detecting the signal emanating from an oxygen-sensitive dye painted on the inside of the glass perifusion chamber. Excitation light was generated and emitted light was detected using 4 Multi Frequency Phase Fluorometers (MFPF-2 Tau Theta, Boulder CO, each unit can detect 2 channels simultaneously), which assessed the oxygen-sensitive signal as the lifetime of the decay of the optical signal in response to the excitation light. The error and drift of this signal was very small (1–2%) and contributed greatly to the stability and accuracy of the measurement system. Data acquisition was driven by the use of a desktop computer with 4 USB ports, and the software supplied by the manufacturer continuously plotted the 8 data graphs in real time.

Mathematical and statistical analysis of kinetic curves. To quantify the effects of drugs on OCR, kinetic responses were fit to a 2-exponential model, where rates of decays were mediated by a mechanism that is either slow or fast. The equation was as follows

$$OCR = OCR_f * \exp(-k_f t) + OCR_s * \exp(-k_s t) \quad (1)$$

where k_f and k_s are rate constants of decay (in units of 1/time), and where OCR_f and OCR_s are the portions of the total initial OCR affected by each decay process. Data were plotted and fit to the model using a non-linear optimization program contained in Kaleidagraph (Synergy Software, Reading, Pennsylvania), which is based on the Levenberg/Marquardt algorithm (Flannery, 1989). Parameter estimates are reported with

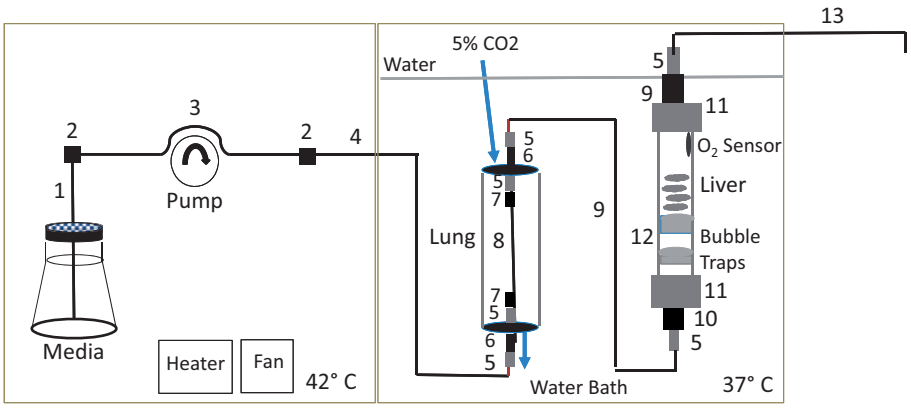

FIG. 1. Schematic of flow culture/assessment system. The components of the environmental housing of the flow system are contained in a plexiglass container (consisting of a left and right compartments that contain the perifusate and is temperature controlled at 42°C by a convective fan and a heating strip (left) and the lung and the perifusion chambers which are submersed in bath water that is temperature controlled at 37°C by an immersion heater (right). The parts of the flow conduit from the pump inflow, through the bubble trap, lung and perifusion chamber to the fraction collector are shown as follows. 1, PEEK Tubing (1/16 × 0.04 × 16 in, 1538XL, IDEX, Lake Forest, Illinois). 2, Conical adaptor, 1/16" to 0.5–0.8 mm union (P-794, IDEX). 3, Tygon pump tubing (Masterflex Tygon E-LFL Tubing, 0.25 mm I.D. × 15 in, 06447-12, Cole-Parmer, Vernon Hills, Illinois). 4, PEEK Tubing (1/16 × 0.04 × 24 in, 1538XL, IDEX). 5, PharMed BPT Tubing (0.8 mm I.D. × 0.75 in, L/S #13, 6508-13, Cole-Parmer). 6, Stainless steel tubing (0.062 (O.D)/0.020 (I.D.) × 1.5 in, (WAT025592, Waters, Milford, Massachusetts). 7, Barbed connector (1/16 to 1/16 in, P-801X, IDEX). 8, Silastic Laboratory Tubing, 0.062 I.D./0.095 O.D. × 10 in, 508-007, Dow Corning, Midland, Michigan). 9, HPFA+ Tubing, 0.062 (O.D.) × 0.02 (I.D.) × 12 in (PM-1451-F, IDEX). 10, Upchurch Scientific Reducer Barbed, 1/16 × 1/8 (P-807X). 11, PharMed BPT Tubing (3.1 mm I.D × 1 in. L/S #16, 6508-16, Cole-Parmer). 12, Frits for bubble trap: porous polyethylene (1/4 in thick, SPEH-4894, Small Parts, Inc, Logansport, Indiana). 13, HPFA+ Tubing, 0.062 (O.D.) × 0.02 (I.D.) × 60 in (PM-1451-F, IDEX). Only 1 channel is shown, but in practice, 8 channels were run at a time.

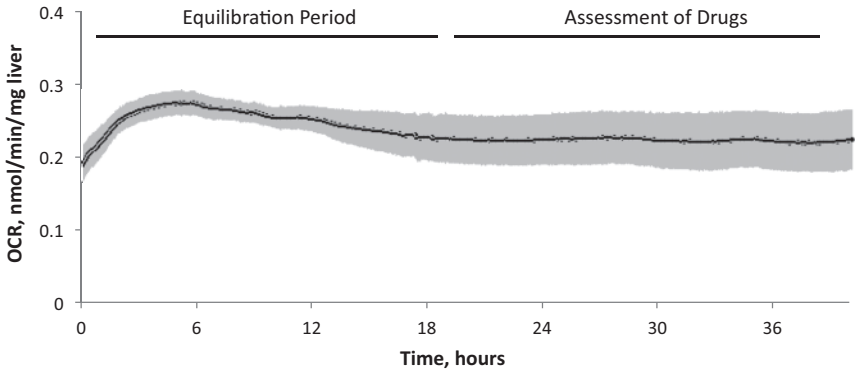

FIG. 2. Kinetic profile of OCR of control liver slices placed in to the flow system immediately after harvesting. Liver slices ($n = 3$ from separate animals done on separate days) were perifused in culture media for 40 h. OCR stabilized after 18–20 h and from then on maintained a very constant value (steady-state values of OCR were 0.22 ± 0.04 nmol/min/mg liver.

standard errors derived from a lack of fit that are calculated by the program.

Error bars on kinetic data reflect the standard error calculated as the standard deviation over the mean divided by square root of the number of replicates. Since the waveforms of the kinetic data were complex, differences in drug effects were evaluated by comparing fitted parameters so that the entire profile was analyzed rather than at single time points. Experiments were done in general to illustrate features of the system, and the numbers of replicates were not typically high enough to reach statistical significance using standard *t*-tests. However in 1 instance (as indicated), the statistical significance of drug effects were evaluated by comparison of the average over the final 15-min interval using a *t*-test.

RESULTS

Optimal Time Window for Testing Drug Exposure

Accurately measuring and properly interpreting small changes in tissue OCR in response to drug exposure requires both a reliable perifusion system and a very stable baseline OCR. Transient effects of tissue isolation would make small decrements difficult to resolve while long-term decrements would indicate unhealthy liver tissue. We routinely achieve such stability as illustrated for a typical experiment in Figure 2 which shows an initial upward drift, followed by a gradual decline in OCR before stabilizing to a steady state level approximately 20 h after liver isolation. We determined that the last 18-h period is the most suitable for assessing subtle drug effects. To further maximize signal-to-noise during this period, we made 2 advances over our previously published methods (Sweet *et al.*, 2002a,b).

Increasing Signal to Noise: Removing Effects of Base Line Drift

Although the variation of oxygen sensor calibration is very small, better methods to control for variations in inflow oxygen content, temperature, barometric pressure, and flow rate of the perifusion media were needed and these were addressed with 2 approaches.

Initially, we corrected for changes of media inflow by measuring both inflow and outflow tensions of oxygen continuously.

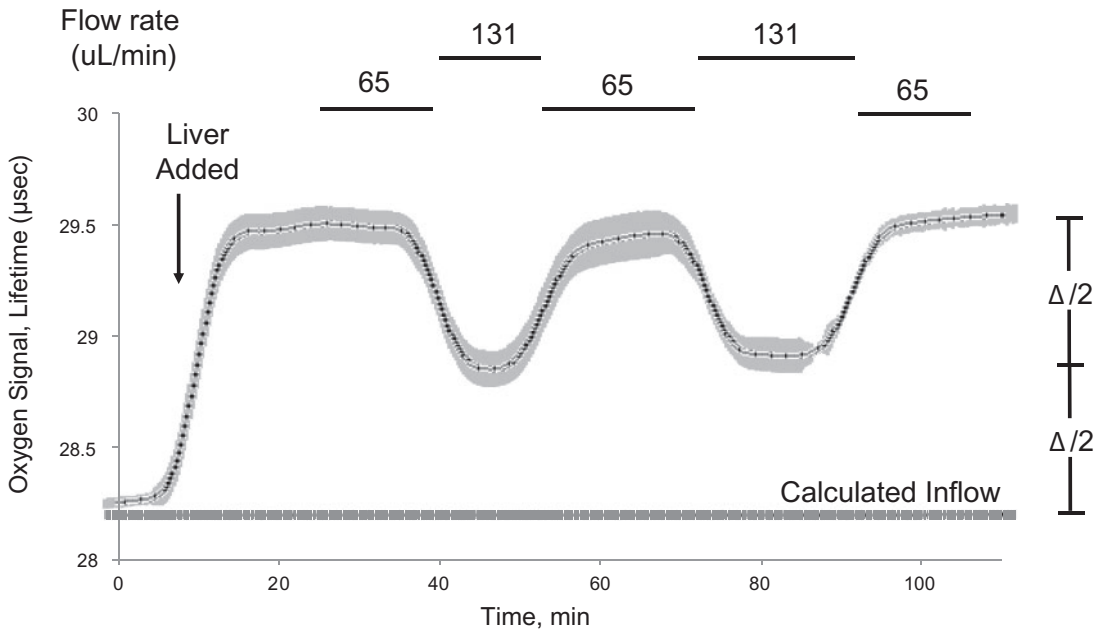

FIG. 3. Determination of inflow concentration of oxygen using periodic flow rate changes. Rather than track the inflow for each individual flow channel and use up available optical detection channels, inflow concentration was determined by periodically doubling the flow rate and calculating the inflow concentration as described in the Methods. Data show the comparison of the calculated value to baseline prior to loading the liver, and subsequent to inhibiting respiration with cyanide.

However, we found it more practical and accurate to measure the difference in oxygen tensions by temporarily altering the flow rate (Fig. 3), typically by doubling it, and calculating the inflow oxygen concentration using the equation

$$OCR = FR \times x(O2_{in} - O2_{out}) \quad (2)$$

for each of the 2 flow rates (FR), and then solving the 2 resulting equations. When carried out in triplicate (as shown in Fig 3), the standard deviation in the estimated inflow oxygen concentration was about 1.5 nmol/ml or about 3% of the typical 50 nmol/ml difference between inflow and outflow oxygen level. (Note that the lifetime of the O_2 lifetime signal is inversely proportional to O_2 tension, which is why increasing the flow rate resulted in a decrease in O_2 lifetime, but increased O_2.) Such flow rate changes were carried out every 18–24 h and the calculated inflow oxygen tension was linearized between determinations.

Our second strategy to control for baseline drift was by perifusing a control chamber in parallel based on the assumption that most factors contributing to drift would affect test and control chambers identically. Thus, OCR profiles obtained in the presence of drugs were normalized to their starting values just prior to drug exposure, and then the normalized data was subtracted from the normalized profiles of the control perfusions (Fig. 4). The control perifusions were typically very stable (less than 5% drift). Subtracting the normalized control signals further increased the resolution of the effects of drug exposure on OCR by effectively removing transient discontinuities. A representative data set for low concentration (0.3 mM) of metformin is shown in Figure 4. The detection limit for the final 12 h of the experiment was about 3%, and the decrement in OCR due to metformin reached the detection limit of 3% after approximately 6 h (Fig. 4, bottom curve) illustrating the increased resolution of low-level OCR that occurs by increasing durations of assessment (Fig. 4). Thus, in the remainder of the results are reported as percent decrements in OCR relative to control.

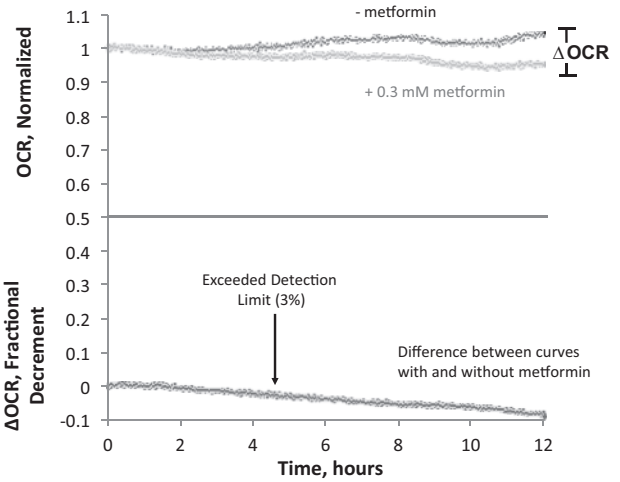

FIG. 4. High resolution of effects of metformin on liver OCR. To maximize the sensitivity to detect low levels of changes in OCR due to the exposure to drugs, the difference between data obtained simultaneously in the presence and absence of 0.3 mM metformin was calculated. This data processing removed the effects of inflow concentration drift and other factors that affected all chambers equally which contributed to short- and long-term noise that ranged around 3%, and increased the resolution of the specific affects of the drug.

We have used these enhanced high-resolution, stable measurement methods to make unprecedented observation of low-concentration drug effects that we suggest may be important evidence for latent drug perturbations not available by conventional toxicity testing methods. We demonstrate these novel capabilities using 2 widely used drugs, metformin, an antidiabetic oral agent, and acetaminophen, an analgesic and antipyretic drug, both of which have been determined to be safe, but have effects on OCR that allows the highlighting of the important features of our method.

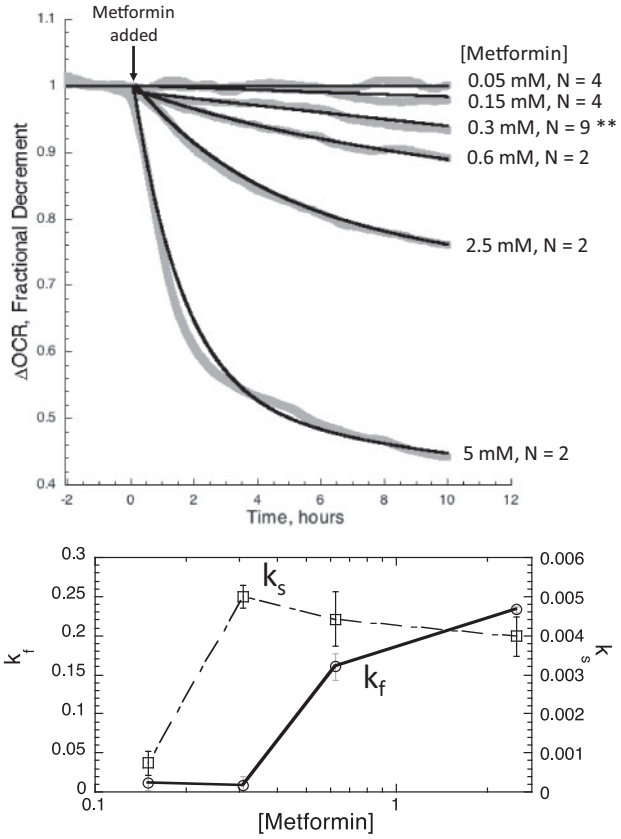

Fig. 5. OCR by rat liver during exposure to various concentrations of metformin. Top, After equilibrating the liver in the flow system for 20 h, metformin was added to the inflow at various concentrations as indicated, and the responses of OCR were continuously assessed during 10 h of drug exposure. The *n* shown for each concentration indicates the number of separate perifusions run on different days using liver slices from different animals. Sufficient replicates were carried out at 0.3 mM metformin ($n = 9$) to run statistical analysis on the OCR decrement average over the final 15 min of the experiment (** denotes $P < .001$). Data were fitted to the multi-exponential decay model (equation 1) for each concentration of metformin. Bottom, Kinetic and dose–response analysis of OCR profiles: distinguishing multiple mechanisms. Values of rate constants for the slow and fast inhibition are plotted as a function of metformin concentration.

High Resolution of Low-Level Perturbations Induced by Metformin

As can be seen in Fig. 5 (Top), the methodological improvements described above allowed us to demonstrate clear time- and concentration-dependent effects of metformin over a 100-fold range of concentrations from 0.05 to 5.0 mM. Six concentrations of metformin were tested per run while the remaining 2 channels were used as controls. A clear effect of 0.15 mM was resolved (Fig. 5 (Bottom)), which is a small percentage of the accepted half-inhibitory concentration (IC_{50}) of 2–4 mM for metformin's inhibition of OCR and well below the 1 mM level which has been undetectable by other cell respiration methods (El-Mir *et al.*, 2000; Silva *et al.*, 2010). To demonstrate reproducibility of the data, we chose 1 concentration where a high enough *n* was carried out to assess statistical significance. At the low dose of 0.3 mM, a decrement of OCR was detected in all 9 liver preparations ranging from 4 to 12%, (mean ± SE, 7.9 ± 1.1%, $P < .001$) demonstrating the high-sensitivity, reproducibility and reliability of our improved assay.

The high-temporal resolution and stability of our methods suggests another important advantage our methods have over currently batch perifusion methods is that we can detect and analyze different drug effect by differences in their kinetics. Kinetic responses to metformin were not adequately fit to a simple, one-exponential decay as might be expected from a single toxicity mechanism. However, the data was nicely described by a 2 exponential model (equation 1) as shown in Fig. 5 (Top), revealing both fast- and slow-exponential decay processes. The low-dose OCR perturbation associated with the slow component of decay had an IC_{50} (≈ 0.3 mM) that was significantly lower than the IC_{50} for the fast component (> 0.6 mM) (Fig. 5 (Bottom); Table 1A).

TABLE 1. Dose Dependency of Fast and Slow Components of Metformin (A) and Acetaminophen (B) Effects

(A) Metformin (mM)	OCR_f	k_f	OCR_s	k_s
0.15	0.095 ± 0.1	0.011 ± 0.01	0.91 ± 0.002	0.0007 ± 0.00031
0.31	0.092 ± 0.1	0.009 ± 0.01	0.9 ± 0.002	0.0055 ± 0.0003
0.625	0.085 ± 0.011	0.16 ± 0.017	0.91 ± 0.012	0.0044 ± 0.0007
2.5	0.24 ± 0.013	0.23 ± 0.004	0.77 ± 0.014	0.004 ± 0.0005
5	0.5 ± 0.001	0.62 ± 0.005	0.52 ± 0.001	0.013 ± 0.0003
(B) Acetaminophen (mM)				
0.165	0.028 ± 0.03	−0.38 ± 0.004	0.97 ± 0.03	0.01 ± 0.0002
0.32	0.034 ± 0.04	−2.8 ± 0.13	0.97 ± 0.03	0.0066 ± 0.0004
0.64	0.1 ± 0.0007	−2.05 ± 0.027	0.92 ± 0.0003	0.0079 ± 0.0007
2.5	0.22 ± 0.0025	−3.17 ± 0.063	0.84 ± 0.0007	0.017 ± 0.0002
5	0.33 ± 0.0021	−4.19 ± 0.044	0.74 ± 0.0005	0.028 ± 0.00014
12.5	0.84 ± 0.006	−3.11 ± 0.04	0.35 ± 0.002	0.0014 ± 0.0012

Equation 1 was fit to the data as shown in Figure 5 (Top) (metformin) and Figure 7 (acetaminophen). Best estimates of the 4 parameters of the model, OCR_f, k_f, OCR_s, and k_s are tabulated plus or minus the standard error. The rate constants k_f and k_s are in units of 1/h and OCR_f and OCR_s are the portions of the total initial OCR affected by each decay process.

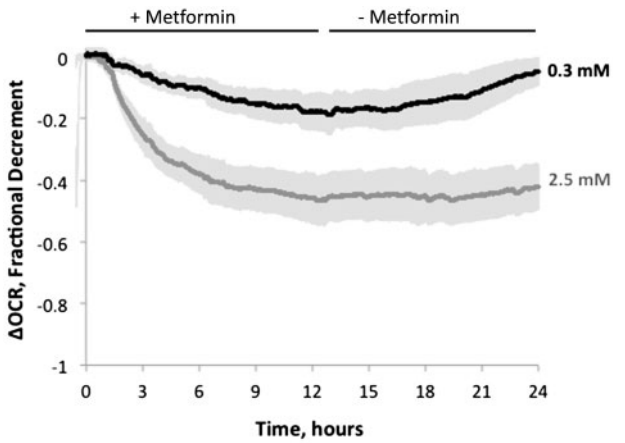

FIG. 6. Reversibility after exposure to 0.3 or 2.5 mM metformin. After exposure to metformin for 10 h, the liver was perifused in the absence of the drug for an additional 12 h. Data are average of 3 separate experiments done on different days and the error bars are plus or minus the SE.

Reversibility of Drug Effects

A further advantage of our continuous long-term perifusion method is the ability to characterize reversibility of drug effects. For example, we measured the reversibility of metformin effects at both the low (0.3 mM) concentration (when only the slow component of decay was activated) and high (2.5 mM) concentration (when both the fast and slow component were activated) (Fig. 6). At the lower concentration of metformin, the modest decrement in OCR was completely reversible, and following removal of the drug the OCR returned to pre-exposure levels. In contrast, at the higher concentration of metformin, the

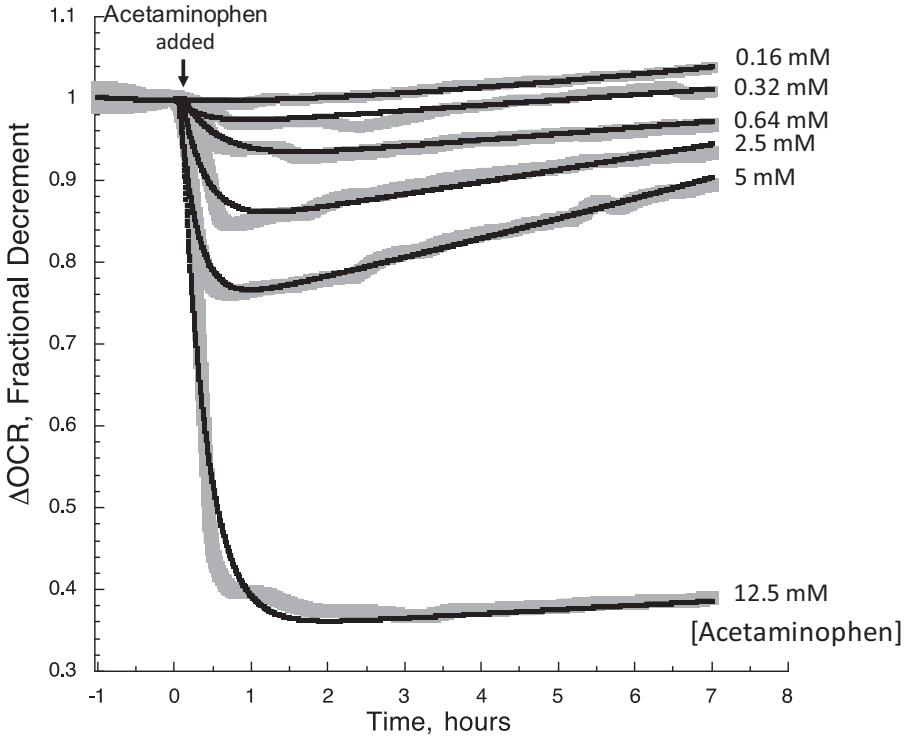

FIG. 7. OCR by rat liver during exposure to various concentrations of acetaminophen. After equilibrating the liver in the flow system for 20 h, the continuous responses to acetaminophen of OCR during 7 h of continuous assessment. Data was fitted to the multiexponential decay model (equation 1) for each concentration of acetaminophen.

decrement in OCR was irreversible during the 12-h washout period. These data suggest that the fast, but not the slow, component is irreversible, supporting the importance of measuring low level perturbations in order to avoid activating low affinity mechanisms that would not occur in clinical settings. It is possible that irreversibility would have to be tested for longer times in order to ensure there was not a slow washout of intracellularly sequestrated drug, and the flow system could be employed to do this.

High Resolution of Low-Level Perturbations Induced by Acetaminophen

As with metformin, clear time- and dose-dependent effects of acetaminophen were observed between 0.32 and 12.5 mM concentrations (Fig. 7). The resolution of effects from 0.32 mM is well below the 3 mM level which has been detectable by other cell respiration methods (Thedinga *et al.*, 2007) and about 2 times pharmacological levels ($C_{max} = 0.07–0.15$ mM, (Kolawole *et al.*, 2002; Malan *et al.*, 1985; Stangier *et al.*, 2000)). At all but the highest concentration tested, the initial decrement in OCR caused by exposure to the drug waned over time (Fig. 7). This indicates that a single time measurement would likely miss that maximum effect and tests of exposure lasting on the order of 6 h or more might not reveal toxic effects of a drug. The data was fit to 2 exponentials, and the dependency of the decrements in OCR on the concentration of acetaminophen was strongly reflected in the magnitude of the fast exponential parameter (OCR_f) (Table 1B). Surprisingly, little change was seen in the parameters reflecting the exponential recovery (OCR_s and k_s) except at 12.5 mM, when no recovery of OCR was observed. The IC_{50} of the overall response (>5 mM) was significantly higher than pharmacological levels of acetaminophen, and typical analysis at the IC_{50} would not provide information relevant to the safety of the drug.

DISCUSSION

Features of the Approach

We have optimized our continuous flow OCR measurement by both minimizing the effects of perifusate flow fluctuations and drift, and establishing an optimal window of stability such that we can measure changes of OCR as small as 5% over 18 h. Our system is suitable for multiple tissue types and does not depend on the introduction and equilibration of exogenous chemical agents (eg, fluorescent dyes) that limit measurement duration. Furthermore, acquisition of real time data over extended periods permits kinetic analysis that can distinguish multiple effects in dose-sensitivity, kinetics and reversibility, as well as the response to simulated drug pharmacokinetic profiles. A key premise and feature of our method is that it provides a global, rather than mechanism-specific, assay of cell function that is sufficiently sensitive to expose unexpected perturbations of cell function whose specific mechanisms warrant further study in the context of pharmaceutical development.

Benefit of measuring drug effects of the full range of concentrations

An important demonstration of our study is that the mechanism of a drug at high concentrations on the order of the IC_{50} for cell death may not be same as those at lower concentrations. High concentrations of metformin induced rapid and irreversible loss of OCR, whereas those below 0.3 mM induced only a slow and fully reversible OCR decrement. Thus, the IC_{50} established by standard toxicity testing exposes mechanisms that are not operative at clinical dose levels while masking a more

clinically relevant low-dose toxicity. The maximal metformin concentration seen in the blood at prescribed doses (C_{max}, about 20 μM) is well below the 150 μM concentration at which we observed detectable decrements in OCR, which is consistent with metformin being a widely used and safe drug. However, the median blood levels during an overdose ranges between 250 μM (median for survivors) and 670 μM (median for nonsurvivors). Clearly, measuring low-level effects of a drug that has some, albeit small, effects on OCR near the C_{max}, and in the ranges of blood values for patients that have undergone an overdose (Dell'Aglio *et al.*, 2009), will be especially useful. Likewise for acetaminophen, one of the most commonly used drugs, the decrement in OCR at C_{max} was undetectable. However, it is also one of the most common drugs to result in toxic effects of the liver (Lee, 2012). This is consistent with the slim margin between the lowest concentration eliciting an observable decrement in OCR and the C_{max} (0.16 vs 0.32 mM), suggesting that only a small excursion of the plasma levels could lead to effects on the liver. Studies are underway on a range of drugs to determine significant decrements in OCR at the C_{max} and to distinguish between harmless and toxic OCR effects.

Effect of the Presence of CO_2 in Media

Our methods use a CO_2-based media, a feature not available in any commercially available system. Bicarbonate and CO_2-aeration are essential for a variety of biochemical processes and functions including gluconeogenesis (Utter and Keech, 1960), fatty acid synthesis in liver (Abu-Elheiga *et al.*, 2001), insulin secretion in pancreatic islets (Henquin and Lambert, 1975, 1976) and the citric acid cycle in muscle (Davis *et al.*, 1980). In general, bicarbonate-buffered culture media are essential for cell growth and maintenance (Ehmann and Misfeldt, 1983; Mitaka *et al.*, 1991). A study on retina observed that without CO_2 buffering, experiments were limited to an experimental duration of about 1.5 h (Adijanto and Philp, 2014).

Comparison of Our Flow Culture System to Static (Nonflowing) OCR Measurement Methods

With the recognition that cellular OCR measures are useful for *in vitro* drug testing (Schoonen *et al.*,2009, 2012; Wang *et al.*, 2015; Wills *et al.*, 2013), other OCR methods are available in static, closed systems in which oxygen depletion is measured within a well-stirred vessel containing a suspension of cells or isolated mitochondria (Jacobus *et al.*, 1982). Although the precision and sensitivity of such systems is good, they are limited by a short duration of OCR measurement (1–2 h at most), and a low throughput (2 experiments can typically be carried out concomitantly). A second type of static system uses an oxygen sensor in each of the closed wells of a multiwell plate to measure OCR. After each determination, wells are opened to refresh the oxygen supply and the measurements are repeated at intervals. The most commonly used system of this design is the commercially available Seahorse extracellular flux analyzer which supports high-throughput analysis of small amounts of biological material (Gerencser *et al.*, 2009), but other such systems have been described (Diepart *et al.*, 2010; Wolf *et al.*, 2013). We anticipate that our flow system's ability to measure precise kinetic waveforms over extended durations will be a powerful complement to the higher throughput methods such as the Seahorse and dye based assays used in high content screening (Attene-Ramos *et al.*, 2013; Diepart *et al.*, 2010).

Metformin's Mechanisms of Action Mediating OCR Decrement

Although real time imaging (Schickinger *et al.*, 2013) for instance with high content screening (O'Brien, 2014) has resolved intracellular events over short durations, accurately measuring the kinetics of sublethal effects likely to occur over a range of hours to days has been difficult. By continuously analyzing the entire modeled pharmacokinetic profile following exposure and removal of the drug, multiple mechanisms of action can be discriminated, and ones that are operational near typical blood levels can be the focus of the *in vitro* analysis. The mechanisms mediating metformin's effect on lowering blood sugar are not well established. Metformin, at high concentrations has been reported to rapidly inhibit Complex 1 in the electron transport chain (El-Mir *et al.*, 2000; Owen *et al.*, 2000). Consistent with this effect, the kinetic response to 2.5 and 5 mM had an inflection point very rapidly following exposure to the drug and dramatically decreased OCR. This was followed by a slower rate of decrease. At lower concentrations, the decrease was steady and linear; notably the slopes of the decrease in OCR after 12 h of exposure to metformin were not very dependent on the drug's concentration. The data are consistent with direct inhibition of the respiratory chain at high levels of metformin, accounting for the rapid and irreversible effect, followed by a second mechanism that induced a slow but reversible loss of OCR, possibly due to a decrease in function and associated ATP usage. A recent report suggests that at concentrations closer to the pharmacological levels, metformin inhibits the redox shuttle enzyme mitochondrial glycerophosphate dehydrogenase, resulting in an altered hepatocellular redox state and decreased hepatic gluconeogenesis (Madiraju *et al.*, 2014). An alternate explanation for metformin's actions was offered, such that the increase in cytosolic NADH may not reflect halting of glycerophosphate shuttle activity, but rather production of NADH by cytosolic glycerophosphate dehydrogenase running in the opposite direction (Baur and Birnbaum, 2014). Irrespective of the mechanism, a decrease in ATP usage due to suppressed gluconeogenesis would be consistent with a reversible decrement in OCR. The data that we obtained cannot support or discredit this explanation. However, the difference in concentration dependency between the fast and slow component of metformin illustrates the point that measuring the toxicity of a drug and extrapolating to what the effects would be at lower concentration is wholly invalid.

Choice of Tissue Model: Rat Liver Slice

Our perfusion apparatus and OCR measurement methods can accommodate many different cell/tissue models including suspended cells (Sahni *et al.*, 2010), attached cell lines (Han *et al.*, 2012), and tissue preparations such as brain slices (Weydt *et al.*, 2006), pancreatic islets (Sweet *et al.*, 2005, 2008), retina (Du *et al.*, 2013) and muscle fibers. For demonstrating applications for drug toxicity testing, we opted for very thin slices of liver that are routinely used as a model for drug toxicity testing (Parrish *et al.*, 1995). The major advantages for this choice are that it is primary tissue, and to some extent the 3-dimensional structure and cell-to-cell interaction is retained. Consistent with other studies (Vickers *et al.*, 2011), the tissue remained viable over 72 h (as assessed by the stability of OCR). Future studies will be carried out on human liver slices, as well as applying the approach to other tissues commonly damaged by drugs including kidney and heart.

Conclusions

We have presented a unique and highly sensitive approach to evaluating effects of drugs on tissue. By use of lifetime detection of oxygen consumption, protocols of extended duration, and taking the difference between the kinetic profiles OCR in the presence and absence of drug, we have achieved an unprecedented sensitivity to resolve drug effects. Importantly we have illustrated that the method can resolve multiple mechanisms mediating drug effects and that measuring at supra-pharmacological levels can activate mechanisms that have no bearing on what occurs at lower, more clinically relevant concentrations. These findings support the critical need for assays with increased sensitivity and highlight the utility of the approach. We predict that the high sensitivity of the method will reveal effects that will be important in the selection of lead compounds, screening of drugs and in the optimization of drug delivery to increase efficacy while minimizing side effects. Thus, our technology is positioned to provide global, early-warning signs of unintended drug effects that may need to be understood and resolved by drug developers. The use of the technology will be further enhanced as we gain understanding of how to distinguish 'safe' effects on mitochondria (perhaps by the criteria of reversibility) from those that ultimately go on to induce cytotoxic effects *in vivo* and we will investigate this in the future by analyzing drugs from the entire range of toxicity levels.

FUNDING

University of Washington Commercialization Gap Fund; National Institutes of Health (R41 TR001196 and the DRC Cell Function Analysis Core (DK17047)); Washington State Life Sciences Discovery Fund (4553677).

REFERENCES

Abu-Elheiga, L., Matzuk, M. M., Abo-Hashema, K. A., and Wakil, S. J. (2001). Continuous fatty acid oxidation and reduced fat storage in mice lacking acetyl-CoA carboxylase 2. *Science* **291**, 2613–2616.

Adijanto, J., and Philp, N. J. (2014). Cultured primary human fetal retinal pigment epithelium (hfRPE) as a model for evaluating RPE metabolism. *Exp. Eye Res.* **126**, 77–84.

Astashkina, A., Mann, B., and Grainger, D. W. (2012). A critical evaluation of in vitro cell culture models for high-throughput drug screening and toxicity. *Pharmacology & Therapeutics* **134**, 82–106.

Baur, J. A., and Birnbaum, M. J. (2014). Control of gluconeogenesis by metformin: does redox trump energy charge? *Cell Metab.* **20**, 197–199.

Davis, E. J., Spydevold, O., and Bremer, J. (1980). Pyruvate carboxylase and propionyl-CoA carboxylase as anaplerotic enzymes in skeletal muscle mitochondria. *Eur. J. Biochem.* **110**, 255–262.

Dell'Aglio, D. M., Perino, L. J., Kazzi, Z., Abramson, J., Schwartz, M. D., and Morgan, B. W. (2009). Acute metformin overdose: examining serum pH, lactate level, and metformin concentrations in survivors versus nonsurvivors: a systematic review of the literature. *Ann. Emerg. Med.* **54**, 818–823.

Diepart, C., Verrax, J., Calderon, P. B., Feron, O., Jordan, B. F., and Gallez, B. (2010). Comparison of methods for measuring oxygen consumption in tumor cells in vitro. *Anal. Biochem.* **396**, 250–256.

Du, J., Cleghorn, W. M., Contreras, L., Lindsay, K., Rountree, A. M., Chertov, A. O., Turner, S. J., Sahaboglu, A., Linton, J., Sadilek, M., *et al.* (2013). Inhibition of mitochondrial pyruvate transport by zaprinast causes massive accumulation of aspartate at the expense of glutamate in the retina. *J. Biol. Chem.* **288**, 36129–36140.

Ehmann, U. K., and Misfeldt, D. S. (1983). CO2/bicarbonate stimulates growth independently of PH in mouse mammary epithelial cells. *In vitro* **19**, 767–774.

El-Mir, M. Y., Nogueira, V., Fontaine, E., Averet, N., Rigoulet, M., and Leverve, X. (2000). Dimethylbiguanide inhibits cell respiration via an indirect effect targeted on the respiratory chain complex I. *J. Biol. Chem.* **275**, 223–28.

Flannery, B. P., Teukolsky, S. A., Vetterling, W. T. (1989). *Numerical Recipes in C*. 2nd ed. Cambridge University Press, Cambridge.

Gerencser, A. A., Neilson, A., Choi, S. W., Edman, U., Yadava, N., Oh, R. J., Ferrick, D. A., Nicholls, D. G., and Brand, M. D. (2009). Quantitative microplate-based respirometry with correction for oxygen diffusion. *Anal. Chem.* **81**, 6868–6878.

Han, C. Y., Umemoto, T., Omer, M., Den Hartigh, L. J., Chiba, T., Leboeuf, R., Buller, C. L., Sweet, I. R., Pennathur, S., Abel, E. D., *et al.* (2012). NADPH oxidase-derived reactive oxygen species increases expression of monocyte chemotactic factor genes in cultured adipocytes. *J. Biol. Chem.* **287**, 10379–10393.

Henquin, J. C., and Lambert, A. E. (1975). Extracellular bicarbonate ions and insulin secretion. *Biochim. Biophys. Acta* **381**, 437–442.

Henquin, J. C., and Lambert, A. E. (1976). Bicarbonate modulation of glucose-induced biphasic insulin release by rat islets. *Am. J. Physiol.* **231**, 713–721.

Jacobus, W. E., Moreadith, R. W., and Vandegaer, K. M. (1982). Mitochondrial respiratory control. Evidence against the regulation of respiration by extramitochondrial phosphorylation potentials or by [ATP]/[ADP] ratios. *J. Biol. Chem.* **257**, 2397–2402.

Kolawole, J. A., Chuhwak, P. D., and Okeniyi, S. O. (2002). Chronopharmacokinetics of acetaminophen in healthy human volunteers. *Eur. J. Drug Metab. Pharmacokinet.* **27**, 199–202.

Lee, W. M. (2012). Acute liver failure. *Semin. Respir. Crit. Care Med.* **33**, 36–45.

Madiraju, A. K., Erion, D. M., Rahimi, Y., Zhang, X. M., Braddock, D. T., Albright, R. A., Prigaro, B. J., Wood, J. L., Bhanot, S., MacDonald, M. J., *et al.* (2014). Metformin suppresses gluconeogenesis by inhibiting mitochondrial glycerophosphate dehydrogenase. *Nature* **510**, 542–546.

Malan, J., Moncrieff, J., and Bosch, E. (1985). Chronopharmacokinetics of paracetamol in normal subjects. *Br. J. Clin. Pharmacol.* **19**, 843–845.

McKim, J. M., Jr. (2010). Building a tiered approach to in vitro predictive toxicity screening: a focus on assays with in vivo relevance. *Comb. Chem. High Throughput Screen.* **13**, 188–206.

Mitaka, T., Sattler, G. L., and Pitot, H. C. (1991). The bicarbonate ion is essential for efficient DNA synthesis by primary cultured rat hepatocytes. *In vitro Cell. Dev. Biol J. Tissue Culture Assoc.* **27A**, 549–556.

O'Brien, P. J. (2014). High-content analysis in toxicology: screening substances for human toxicity potential, elucidating subcellular mechanisms and in vivo use as translational safety biomarkers. *Basic Clin. Pharmacol. Toxicol.* **115**, 4–17.

Parrish, A. R., Gandolfi, A. J., and Brendel, K. (1995). Precision-cut tissue slices: applications in pharmacology and toxicology. *Life Sci.* **57**, 1887–1901.

Sahni, J., Tamura, R., Sweet, I. R., and Scharenberg, A. M. (2010). TRPM7 regulates quiescent/proliferative metabolic transitions in lymphocytes. *Cell Cycle* **9**, 12798.

Schickinger, S., Bruns, T., Wittig, R., Weber, P., Wagner, M., and Schneckenburger, H. (2013). Nanosecond ratio imaging of redox states in tumor cell spheroids using light sheet-based fluorescence microscopy. *J. Biomed. Optics* **18**, 126007.

Schoonen, W. G., Stevenson, J. C., Westerink, W. M., and Horbach, G. J. (2012). Cytotoxic effects of 109 reference compounds on rat H4IIE and human HepG2 hepatocytes. III: Mechanistic assays on oxygen consumption with MitoXpress and NAD(P)H production with Alamar Blue. *Toxicol. In Vitro* **26**, 511–525.

Schoonen, W. G., Westerink, W. M., and Horbach, G. J. (2009). High-throughput screening for analysis of in vitro toxicity. *Exs* **99**, 401–452.

Silva, F. M., da Silva, M. H., Bracht, A., Eller, G. J., Constantin, R. P., and Yamamoto, N. S. (2010). Effects of metformin on glucose metabolism of perfused rat livers. *Mol Cell Biochem.* **340**, 283–289.

Stangier, J., Su, C. A., Fraunhofer, A., and Tetzloff, W. (2000). Pharmacokinetics of acetaminophen and ibuprofen when coadministered with telmisartan in healthy volunteers. *J. Clin. Pharmacol.* **40**, 1338–13346.

Sweet, I. R., Cook, D. L., DeJulio, E., Wallen, A. R., Khalil, G., Callis, J., and Reems, J. (2004). Regulation of ATP/ADP in pancreatic islets. *Diabetes* **53**, 401–409.

Sweet, I. R., Cook, D. L., Wiseman, R. W., Greenbaum, C. J., Lernmark, A., Matsumoto, S., Teague, J. C., and Krohn, K. A. (2002a). Dynamic perifusion to maintain and assess isolated pancreatic islets. *Diabetes Technol. Ther.* **4**, 67–76.

Sweet, I. R., and Gilbert, M. (2006). Contribution of calcium influx in mediating glucose-stimulated oxygen consumption in pancreatic islets. *Diabetes* **55**, 3509–3519.

Sweet, I. R., Gilbert, M., Jensen, R., Sabek, O., Fraga, D. W., Gaber, A. O., and Reems, J. (2005). Glucose stimulation of cytochrome C reduction and oxygen consumption as assessment of human islet quality. *Transplantation* **80**, 1003–1011.

Sweet, I. R., Gilbert, M., Scott, S., Todorov, I., Jensen, R., Nair, I., Al-Abdullah, I., Rawson, J., Kandeel, F., and Ferreri, K. (2008). Glucose-stimulated increment in oxygen consumption rate as a standardized test of human islet quality. *Am. J. Transplant.* **8**, 183–92.

Sweet, I. R., Khalil, G., Wallen, A. R., Steedman, M., Schenkman, K. A., Reems, J. A., Kahn, S. E., and Callis, J. B. (2002b). Continuous measurement of oxygen consumption by pancreatic islets. *Diabetes Technol. Ther.* **4**, 661–672.

Thedinga, E., Ullrich, A., Drechsler, S., Niendorf, R., Kob, A., Runge, D., Keuer, A., Freund, I., Lehmann, M., and Ehret, R. (2007). In vitro system for the prediction of hepatotoxic effects in primary hepatocytes. *Altex* **24**, 22–34.

Utter, M. F., and Keech, D. B. (1960). Formation of oxaloacetate from pyruvate and carbon dioxide. *J. Biol. Chem.* **235**, PC17–PC18.

Vickers, A. E., Fisher, R., Olinga, P., and Dial, S. (2011). Repair pathways evident in human liver organ slices. *Toxicol. In Vitro* **25**, 1485–1492.

Wang, R., Novick, S. J., Mangum, J. B., Queen, K., Ferrick, D. A., Rogers, G. W., and Stimmel, J. B. (2015). The acute extracellular flux (XF) assay to assess compound effects on mitochondrial function. *J. Biomol. Screen* **20**, 422–429.

Weydt, P., Pineda, V. V., Torrence, A. E., Libby, R. T., Satterfield, T. F., Lazarowski, E. R., Gilbert, M. L., Morton, G. J., Bammler, T. K., Strand, A. D., *et al.* (2006). Thermoregulatory and metabolic defects in Huntington's disease transgenic mice implicate PGC-1alpha in Huntington's disease neurodegeneration. *Cell Metab.* **4**, 349–362.

Wills, L. P., Beeson, G. C., Trager, R. E., Lindsey, C. C., Beeson, C. C., Peterson, Y. K., and Schnellmann, R. G. (2013). High-throughput respirometric assay identifies predictive toxicophore of mitochondrial injury. *Toxicol. Appl. Pharmacol.* **272**, 490–502.

Wolf, P., Brischwein, M., Kleinhans, R., Demmel, F., Schwarzenberger, T., Pfister, C., and Wolf, B. (2013). Automated platform for sensor-based monitoring and controlled assays of living cells and tissues. *Biosensors Bioelectron.* **50**, 111–117.

Zemmel, R., and Sheikh, M. (2010). McKinsey & Company. Invention reinvented: McKinsey perspectives on pharmaceutical R & D.